



PESARO 2023

The Thirteenth International Conference on Performance, Safety and Robustness
in Complex Systems and Applications

ISBN: 978-1-68558-039-1

April 24th – 28th, 2023

Venice, Italy

PESARO 2023 Editors

Lorena Parra Boronat, Universitat Politecnica de Valencia, Spain

PESARO 2023

Forward

The Thirteenth International Conference on Performance, Safety and Robustness in Complex Systems and Applications (PESARO 2023), held between April 24th and April 28th, 2023, continued a series of events dedicated to fundamentals, techniques and experiments to specify, design, and deploy systems and applications under given constraints on performance, safety and robustness.

There is a relation between organizational, design and operational complexity of organization and systems and the degree of robustness and safety under given performance metrics. More complex systems and applications might not necessarily be more profitable, but are less robust. There are trade-offs involved in designing and deploying distributed systems. Some design technologies have a positive influence on safety and robustness, even operational performance is not optimized. Under constantly changing system infrastructure and user behaviors and needs, there is a challenge in designing complex systems and applications with a required level of performance, safety and robustness.

We take here the opportunity to warmly thank all the members of the PESARO 2023 technical program committee, as well as all the reviewers. The creation of such a high-quality conference program would not have been possible without their involvement. We also kindly thank all the authors who dedicated much of their time and effort to contribute to PESARO 2023. We truly believe that, thanks to all these efforts, the final conference program consisted of top-quality contributions. We also thank the members of the PESARO 2023 organizing committee for their help in handling the logistics of this event.

We hope that PESARO 2023 was a successful international forum for the exchange of ideas and results between academia and industry and for the promotion of progress in the areas of performance, safety, and robustness of complex systems and applications.

PESARO 2023 Chairs

PESARO 2023 Steering Committee

Mohammad Rajabali Nejad, University of Twente, the Netherlands
Rémy Houssin, Université de Strasbourg - ICube Laboratory, France
Yulei Wu, University of Exeter, UK
Wolfgang Leister, Norsk Regnesentral, Norway

PESARO 2023 Publicity Chairs

Laura Garcia, Universitat Politecnica de Valencia, Spain
Javier Rocher Morant, Universitat Politecnica de Valencia, Spain

PESARO 2023 Committee

PESARO 2023 Steering Committee

Mohammad Rajabali Nejad, University of Twente, the Netherlands
Rémy Houssin, Université de Strasbourg - ICube Laboratory, France
Yulei Wu, University of Exeter, UK
Wolfgang Leister, Norsk Regnesentral, Norway

PESARO 2023 Publicity Chairs

Laura Garcia, Universitat Politecnica de Valencia, Spain
Javier Rocher Morant, Universitat Politecnica de Valencia, Spain

PESARO 2023 Technical Program Committee

H. B. Acharya, Rochester Institute of Technology, USA
Mohammad AlMasri, Nvidia, USA
Kaustav Basu, Arizona State University, USA
Morteza Biglari-Abhari, University of Auckland, New Zealand
Chérifa Boucetta, University of Reims Champagne Ardenne, France
Lelio Campanile, University of Campania Luigi Vanvitelli, Italy
Pasquale Cantiello, University of Campania Luigi Vanvitelli, Italy
Frank Coolen, Durham University, UK
Faten Fakhfakh, National School of Engineering of Sfax, Tunisia
Victor Flores, Universidad Católica del Norte, Chile
Rita Girao-Silva, University of Coimbra & INESC-Coimbra, Portugal
Marco Gribaudo, Politecnico di Milano, Italy
Mohamed-Faouzi Harkat, Badji Mokhtar - Annaba University, Algeria
Christoph-Alexander Holst, inIT - Institute Industrial IT, Germany
Rémy Houssin, Université de Strasbourg - ICube Laboratory, France
Benoit Iung, Lorraine University, France
Christos Kalloniatis, University of the Aegean, Greece
Atsushi Kanai, Hosei University, Japan
Liuwang Kang, University of Virginia, USA
Sokratis K. Katsikas, Norwegian University of Science and Technology, Norway
Georgios Keramidas, Think Silicon S.A., Greece
Michel A. Kinsy, STAM Center | Arizona State University, USA
Vincent Latzko, Technische Universität Dresden, Germany
Wolfgang Leister, Norsk Regnesentral, Norway
Lúcia Martins, University of Coimbra, Portugal
Michele Mastroianni, University of Campania -Luigi Vanvitelli, Italy
Ilaria Matteucci, IIT-CNR, Italy
Mohamed Nidhal Mejri, Paris 13 University, France
Weizhi Meng, Technical University of Denmark, Denmark

Andrey Morozov, University of Stuttgart | Institute of Industrial Automation and Software Engineering (IAS), Germany

Mohammad Rajabali Nejad, University of Twente, the Netherlands

Mohamed Nounou, Texas A&M University at Qatar, Qatar

Tuan Phung-Duc, University of Tsukuba, Japan

Vladimir Podolskiy, Technical University of Munich, Germany

Asad Ur Rehman, Instituto de Telecomunicações, Portugal

Jean-Pierre Seifert, TU Berlin & FhG SIT Darmstadt, Germany

Omar Smadi, Iowa State University, USA

Kumiko Tadano, NEC Corporation, Japan

Eirini Eleni Tsiropoulou, University of New Mexico, USA

Yulei Wu, University of Exeter, UK

Bingyi Zhang, University of Southern California, USA

Piotr Zwierzykowski, Poznan University of Technology, Poland

Copyright Information

For your reference, this is the text governing the copyright release for material published by IARIA.

The copyright release is a transfer of publication rights, which allows IARIA and its partners to drive the dissemination of the published material. This allows IARIA to give articles increased visibility via distribution, inclusion in libraries, and arrangements for submission to indexes.

I, the undersigned, declare that the article is original, and that I represent the authors of this article in the copyright release matters. If this work has been done as work-for-hire, I have obtained all necessary clearances to execute a copyright release. I hereby irrevocably transfer exclusive copyright for this material to IARIA. I give IARIA permission to reproduce the work in any media format such as, but not limited to, print, digital, or electronic. I give IARIA permission to distribute the materials without restriction to any institutions or individuals. I give IARIA permission to submit the work for inclusion in article repositories as IARIA sees fit.

I, the undersigned, declare that to the best of my knowledge, the article does not contain libelous or otherwise unlawful contents or invading the right of privacy or infringing on a proprietary right.

Following the copyright release, any circulated version of the article must bear the copyright notice and any header and footer information that IARIA applies to the published article.

IARIA grants royalty-free permission to the authors to disseminate the work, under the above provisions, for any academic, commercial, or industrial use. IARIA grants royalty-free permission to any individuals or institutions to make the article available electronically, online, or in print.

IARIA acknowledges that rights to any algorithm, process, procedure, apparatus, or articles of manufacture remain with the authors and their employers.

I, the undersigned, understand that IARIA will not be liable, in contract, tort (including, without limitation, negligence), pre-contract or other representations (other than fraudulent misrepresentations) or otherwise in connection with the publication of my work.

Exception to the above is made for work-for-hire performed while employed by the government. In that case, copyright to the material remains with the said government. The rightful owners (authors and government entity) grant unlimited and unrestricted permission to IARIA, IARIA's contractors, and IARIA's partners to further distribute the work.

Table of Contents

Energy-Efficient Resource Allocation Algorithm in the UAV-enabled Data and Energy Integrated Network <i>Yang Wang and Kun Yang</i>	1
---	---

Energy-Efficient Resource Allocation Algorithm in the UAV-enabled Data and Energy Integrated Network

Yang Wang

School of Information and Communication Engineering
University of Electronic Science and Technology of China
Chengdu, Sichuan, China
email: yw@std.uestc.edu.cn

Kun Yang

School of Information and Communication Engineering
University of Electronic Science and Technology of China
Chengdu, Sichuan, China
email: kunyang@uestc.edu.cn

Abstract—This paper considers a new Data and Energy Integrated Network (DEIN), which conceives an Unmanned Aerial Vehicle (UAV) and numerable Internet of Things (IoT) devices on the ground. The UAV is capable of transmitting data and energy to the IoT devices. The UAV in the air wirelessly charges the IoT devices with Wireless Power Transfer (WPT) technology, and the IoT devices start Wireless Information Transfer (WIT) after the charging process. In this paper, the channel model and data and energy transmission model between the UAV and IoT devices are established. In order to minimize the total energy consumption of the UAV, this paper proposes an energy-efficient resource allocation algorithm by jointly optimizing of the trajectory of the UAV, the communication scheduling and charging fraction of the IoT devices on the ground. Successive convex approximation and block coordinate descent algorithm are introduced in this paper to address the optimization problem. Both the effectiveness and the efficiency of the proposed joint optimization algorithm have been validated with the simulation.

Keywords—Data and Energy Integrated Network (DEIN); Unmanned Aerial Vehicle (UAV); Internet of Things (IoT); Wireless Power Transfer (WPT); Wireless Information Transfer (WIT).

I. INTRODUCTION

With the rapid development of science and technology, the Internet of Things has been everywhere and has effectively improved people's production and life in many areas like industrial and agricultural production, oil and gas field exploration and acquisition and so on [1]. With the widespread deployment and use of IoT devices, these IoT devices are always working. For example, the IoT sensors continue collecting and uploading data [2], and the energy consumption keeps increasing [3]. Therefore, the energy consumption of the Internet of Things has become a big challenge for its future development.

This paper considers a new type of IoT network, which consists of a mobile base station and multiple fixed battery-free IoT devices. The mobile base station in this paper mainly refers to UAV. Due to the advantages of high flexibility and low cost, UAVs have been widely used in agriculture, industry, military and other fields [4] [5]. As a mobile base station, the UAV can act as a flexible communication platform in the air to collect and process data from ground devices [6]. Many researchers have deployed UAVs appropriately to achieve seamless coverage of the target environment. The throughput of the wireless networks can be improved a lot [7]–

[9]. The performance of the network can be further improved by optimizing the trajectory of the UAV [10] [11]. However, most of the literatures mainly consider the improvement of the communication performance of the system by UAV, and few of them consider the system energy supply by UAV. In addition to WIT, the UAV considered in this paper also supports WPT technology [12], which can be used to wirelessly charge IoT devices and provide energy for IoT devices in remote or complex environments [13]. Under such background, this paper considers the UAV supporting both WIT and WPT. The UAV can charge the ground IoT devices with WPT technology [14] and collect data from them. Although this paper assumes that the energy of the UAV is sufficient for its working task, the energy consumption of the UAV will have a great impact on the overall performance of the system, which cannot be ignored. Therefore, this paper aims to minimize the overall energy consumption of the UAV by jointly optimizing the UAV's flight trajectory and the IoT devices' communication scheduling and charging fractions.

The remainder of this paper is organized as follows. In Section II, the system model is established in detail and the energy consumption minimization problem is formulated. The optimization problem is solved in Section III. On top of that, the proposed energy-efficient resource allocation algorithm aiming to minimize the energy consumption of the UAV is designed and clarified in detail. The performance evaluation based on simulation experiments is presented in Section IV. Finally, this paper concludes in Section V.

II. SYSTEM MODEL AND PROBLEM FORMULATION

The wireless data and energy transmission system based on mobile base station is shown in the Figure 1. This system is mainly composed of one UAV flying in the air and several IoT devices with fixed positions on the ground. The UAV flies over these IoT devices according to a certain trajectory. The radio front of the UAV is a directional antenna fixed on a 2-DOF Pan-tilt. The horizontal and vertical direction of the antenna can be freely adjusted according to the position of the target charging device. Thus, the UAV can aim at the target charging device for directional wireless energy transmission with high charging efficiency. The radio front of all the IoT devices on the ground is a fixed omnidirectional antenna. By default, all

IoT devices on the ground are always in a dormant state. In each time slot, only one device is served by the UAV. The corresponding device only wakes up when the UAV transmits radio frequency (RF) energy to it in a certain time slot. After the wireless charging is completed, the IoT device will upload its data to the UAV.

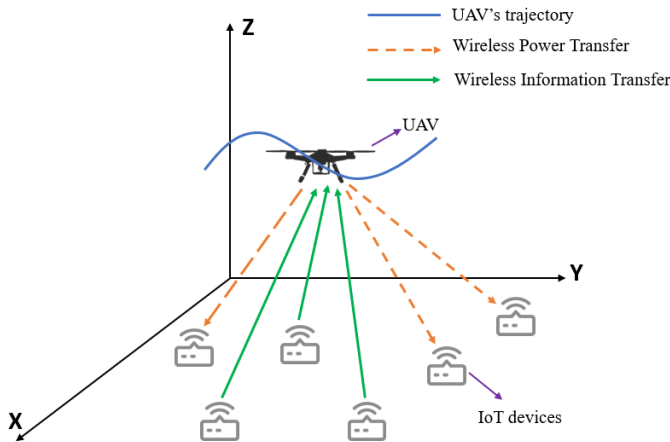


Figure 1. UAV-enabled data and energy integrated network.

In this section, the total number of all the IoT devices is denoted as K , so the number set of all the IoT devices is denoted as $\mathcal{K} = \{1, 2, \dots, K\}$. Thus, the set of all the IoT devices can be denoted as $\mathbf{UE} = \{UE_k | \forall k \in \mathcal{K}\}$. This paper assumes that during a complete UAV flight cycle, the UAV takes off from its starting position and returns to its starting position when the flight is over. Consequently, a closed-loop flight trajectory is formed. For the convenience of problem-formulation and problem-solving, the continuous flight trajectory of UAV is discretely processed in this paper. The flight cycle of UAV is set as a constant, which is denoted as T . The trajectory of the UAV during the whole flight cycle is divided into M points, which all have same duration of time. Thus, the M time slots have same duration of time $\Delta\tau = \frac{T}{M}$. When the length of each time slot $\Delta\tau$ is set sufficiently small, it can be approximately considered that the position of the UAV will not change within this time slot. In this paper, all time slots in a flight cycle of UAV are numbered, so the set of all time slot numbers can be denoted as $\mathcal{M} = \{1, 2, \dots, M\}$ and the set of all timeslots can be denoted as $\mathbf{Slot} = \{\text{Slot}_t | \forall t \in \mathcal{M}\}$. To sum up, the UAV flight trajectory is discretized into M positions, and the path of the entire flight cycle can be obtained by solving the problem of the UAV position within M time slots.

A. Wireless Communication Model

The position of the UAV is represented by 3D Cartesian coordinate system, as shown below.

$$[\mathbf{q}(t), H]^T, \mathbf{q}(t) = [x(t), y(t)], \forall t \in \mathcal{M} \quad (1)$$

where $\mathbf{q}(t) \in \mathbb{R}^{1 \times 2}$ denotes the coordinate of the UAV in Slot_t . H denotes the flight altitude of the UAV in Slot_t and it's

set as a constant in this paper. $[\bullet]^T$ represents the transposition of the matrix. Similarly, the IoT devices on the ground can be represented as follows.

$$[\mathbf{w}_k, 0]^T, \mathbf{w}_k = [x_k, y_k], \forall k \in \mathcal{K} \quad (2)$$

where $\mathbf{w}_k \in \mathbb{R}^{1 \times 2}$ denotes the horizontal coordinate of UE_k . The altitude of all the IoT devices on the ground is set to 0. The free space path loss model is adopted in this paper since the UAV is at a certain altitude during each working cycle, which mainly considers the Line of Sight (LoS) communication and transmission link between the UAV and the ground IoT devices. The channel gain mainly depends on the distance between the UAV and the IoT devices on the ground. According to the UAV and the IoT devices' coordinates, the distance between the UAV and the corresponding UE_k in Slot_t can be represented as follows.

$$d_k(t) = \sqrt{\|\mathbf{q}(t) - \mathbf{w}_k\|^2 + H^2}, \forall k \in \mathcal{K}, t \in \mathcal{M} \quad (3)$$

The channel gain between the UAV and the corresponding UE_k in Slot_t can be represented as:

$$h_k(t) = \frac{\beta_0}{d_k^2(t)} = \frac{\beta_0}{\|\mathbf{q}(t) - \mathbf{w}_k\|^2 + H^2}, \forall k \in \mathcal{K}, t \in \mathcal{M} \quad (4)$$

where β_0 denotes the channel power gain when the reference distance is set to 1 meter. Consequently, it can be seen that the channel gain varies in different time slots, and it is assumed that the channel gain remains unchanged in the same time slot.

A binary variable is defined to represent the scheduling of the IoT devices on the ground, which is denoted as $a_k(t)$. Thus, it meets the following condition:

$$a_k(t) = \{0, 1\}, \forall k \in \mathcal{K}, t \in \mathcal{M} \quad (5)$$

$a_k(t)$ represents the scheduling variable of UE_k in Slot_t , where $a_k(t) = 1$ represents the UE_k is first wirelessly charged by the UAV and uploads data to the UAV in Slot_t . On the contrary, it means the UE_k is not served by the UAV in Slot_t when $a_k(t) = 0$. This paper assumes that in each time slot, only one UE can be served by UAV. Therefore $a_k(t)$ should be subject to (6):

$$\sum_{k=1}^K a_k(t) \leq 1, \forall t \in \mathcal{M} \quad (6)$$

Besides, the variable of charging proportion is defined to represent the charging time allocation of the IoT device when it is scheduled. It is denoted as $\xi_k(t)$ and meets the following condition:

$$0 \leq \xi_k(t) \leq 1, \forall k \in \mathcal{K}, t \in \mathcal{M} \quad (7)$$

Equation (7) represents the charging proportion of UE_k in Slot_t . Thus, the proportion of data uploading can be obtained as $1 - \xi_k(t)$. $\xi_k(t) = 0$ means UE_k only uploads data to the UAV but without being charged by the UAV in Slot_t . On the other hand, $\xi_k(t) = 1$ means UE_k spends all the time of Slot_t on harvesting wireless energy transmitted from the UAV but without uploading data to the UAV. According to the classic

Shannon's channel capacity equation, the achievable data rate of UE_k in $Slot_t$ can be formulated as (8):

$$r_k(t) = B \log_2 \left(1 + \frac{P_k \beta_0}{(\|\mathbf{q}(t) - \mathbf{w}_k\|^2 + H^2) \sigma^2} \right), \quad (8)$$

$$\forall k \in \mathcal{K}, t \in \mathcal{M}$$

where B represents the bandwidth of wireless channel, P_k represents the transmission power of data uploading of UE_k in $Slot_t$, and σ^2 represents the noise power at the signal receiver of the UAV. D_k is defined as the total data transmission requirements of UE_k during the whole flight cycle of the UAV. These data is cached in the buffer area of the device. It is assumed that the UE_k needs to complete the data transmission task before the end of a flight cycle of the UAV, and the constraint of data transmission can be obtained as (9):

$$\sum_{t=1}^M a_k(t) r_k(t) (1 - \xi_k(t)) \Delta\tau \geq D_k, \forall k \in \mathcal{K} \quad (9)$$

B. Energy Consumption Model of IoT devices

The power of wireless charging from the UAV to the IoT devices on the ground is assumed as constant, which is denoted as P_U . Within any time slot, when the designated IoT device is scheduled and the corresponding wireless charging proportion variable is non-zero, the UAV will wirelessly transmit RF energy to this device in this time slot. In $Slot_m$, the total energy received by UE_k can be formulated as (10):

$$E_k(m) = \sum_{t=1}^m \frac{\eta \beta_0 a_k(t) P_U \xi_k(t) \Delta\tau}{\|\mathbf{q}(t) - \mathbf{w}_k\|^2 + H^2}, \forall k \in \mathcal{K}, m \in \mathcal{M} \quad (10)$$

where η represents the conversion efficiency of the UE to convert the received RF signal into DC electric energy that can be directly utilized by the load. It is set to a constant in this paper. In order to ensure UE_k has enough energy for data uploading, its energy reception and consumption should meet the energy constraint (11) in $Slot_m$.

$$E_k(m) - \sum_{t=1}^m a_k(t) (1 - \xi_k(t)) P_k \Delta\tau \geq \varepsilon_k, \forall k \in \mathcal{K}, m \in \mathcal{M} \quad (11)$$

where ε_k is a constant to ensure UE_k has sufficient residual energy.

C. Energy Consumption Model of the UAV

The energy consumption of UAV mainly includes two parts: the energy consumed by its own flight and the energy consumed by wireless charging for the ground energy IoT device. The energy consumed by UAV within a complete flight cycle [15] can be expressed as (12):

$$E_f = \sum_{t=1}^M \Delta\tau \left(\frac{1}{2} d_0 \rho s G (\nu_h(t))^3 + P_0 \left(1 + \frac{3(\nu_h(t))^2}{U_{tip}^2} \right) + P_1 \left(\sqrt{1 + \frac{(\nu_h(t))^4}{4(\nu_0)^4}} - \frac{(\nu_h(t))^2}{2(\nu_0)^2} \right)^{\frac{1}{2}} + P_2 \nu_v(t) \right) \quad (12)$$

where d_0 , ρ , s and G respectively represent the fuselage resistance ratio of the UAV, the air density, the rotor stiffness of

the UAV and the rotor disk area of the UAV. $\nu_h(t)$ and $\nu_v(t)$ respectively represent the horizontal flight speed and vertical flight speed of the UAV in $Slot_t$. P_0 , P_1 and P_2 respectively represent the blade profile power, induction power of the UAV and constants related to the vertical flight of the UAV. U_{tip} represents the tip speed of the UAV's rotor blade. ν_0 represents the rotor induced velocity while the UAV is hovering.

In the scenario of data and energy transmission between the UAV and the ground IoT device considered in this paper, since the altitude of the UAV is assumed to be constant, the vertical flight speed of UAV in $Slot_t$ obeys $\nu_v(t) = 0$. As a consequence, the energy consumed by UAV within a complete flight cycle can be re-expressed as (13).

$$E_f = \sum_{t=1}^M \Delta\tau \left(\frac{1}{2} d_0 \rho s G (\nu_h(t))^3 + P_0 \left(1 + \frac{3(\nu_h(t))^2}{U_{tip}^2} \right) + P_1 \left(\sqrt{1 + \frac{(\nu_h(t))^4}{4(\nu_0)^4}} - \frac{(\nu_h(t))^2}{2(\nu_0)^2} \right)^{\frac{1}{2}} \right) \quad (13)$$

where the horizontal flight speed of the UAV in $Slot_t$ is defined as $\nu_h(t) = \frac{\|\mathbf{q}(t) - \mathbf{q}(t-1)\|}{\Delta\tau}$. In a complete flight cycle of the UAV, the energy E_c consumed by wireless charging for the ground IoT device can be expressed as (14):

$$E_c = \sum_{t=1}^M \sum_{k=1}^K a_k(t) \xi_k(t) P_U \Delta\tau \quad (14)$$

Therefore, the total energy consumed by the UAV in a complete flight cycle can be obtained by combining (13) and (14). It is re-expressed in (15):

$$E_{cons} = E_f + E_c \quad (15)$$

D. Problem formulation

It is assumed in this paper that the initial energy of UAV at the beginning of each flight cycle is sufficient to meet all the energy consumption requirements in a whole flight cycle. According to the description of the above system model, the optimization problem of minimizing the energy consumption of the mobile data and energy base station (UAV) studied in this paper can be formulated as follows:

$$\min_{Q, A, \Xi} E_{cons} \quad (16)$$

$$s.t. a_k(t) = \{0, 1\}, \forall k \in \mathcal{K}, t \in \mathcal{M} \quad (16a)$$

$$\sum_{k=1}^K a_k(t) \leq 1, \forall t \in \mathcal{M} \quad (16b)$$

$$0 \leq \xi_k(t) \leq 1, \forall k \in \mathcal{K}, t \in \mathcal{M} \quad (16c)$$

$$\sum_{t=1}^M a_k(t) r_k(t) (1 - \xi_k(t)) \Delta\tau \geq D_k, \forall k \in \mathcal{K} \quad (16d)$$

$$E_k(m) - \sum_{t=1}^m a_k(t) (1 - \xi_k(t)) P_k \Delta\tau \geq \varepsilon_k, \forall k \in \mathcal{K}, m \in \mathcal{M} \quad (16e)$$

$$\|\mathbf{q}(t) - \mathbf{q}(t-1)\| \leq \nu_{h,max} \Delta\tau, \forall t \in \mathcal{M} \quad (16f)$$

The optimization objective of the above problem is to minimize the total energy consumption of the UAV in a single flight cycle by jointly optimizing the flight trajectory of the UAV, the scheduling variables and the wireless charging ratio of the ground IoT device. The three optimization variables $\mathbf{Q} = \{\mathbf{q}(t), t \in \mathcal{M}\}$, $\mathbf{A} = \{a_k(t), k \in \mathcal{K}, t \in \mathcal{M}\}$, $\Xi = \{\xi_k(t), k \in \mathcal{K}, t \in \mathcal{M}\}$ respectively represent the flight trajectory of the UAV in the horizontal direction, the scheduling set and the charging proportion set of all ground data and energy IoT device. $\mathcal{K} = \{1, 2, \dots, K\}$ is a set of numbers of all ground devices, and $\mathcal{M} = \{1, 2, \dots, M\}$ is a set of numbers of all time slots during a UAV flight cycle. Equation (16a) and (16b) are constraints on communication scheduling variables of the ground IoT device. Equation (16c) is the numerical range of wireless charging ratio of all the IoT device. Equation (16d) is the data requirement constraint for uplink transmission of each IoT device. Equation (16e) is the energy constraint of each IoT device. Equation (16f) is the limit of the UAV's horizontal flight speed ($\nu_{h,max}$ represents the maximum flight speed of UAV in the horizontal direction).

III. PROPOSED SOLUTION

It can be seen that the optimization problem (16) is a mixed-integer non-convex problem. Next, the problem (16) is decomposed into three subproblems to solve.

A. Optimization of the UAV's Trajectory

For any given and feasible communication scheduling $A = \{a_k(t), k \in \mathcal{K}, t \in \mathcal{M}\}$ and charging fractions $\Xi = \{\xi_k(t), k \in \mathcal{K}, t \in \mathcal{M}\}$, energy consumption of the UAV in a whole flight period for wireless charging E_c is a constant. Thus, the subproblem of optimizing the UAV's trajectory is formulated as (17).

$$\min_{\mathbf{Q}} E_f \quad (17)$$

$$s.t. \sum_{t=1}^M a_k(t) r_k(t) (1 - \xi_k(t)) \Delta\tau \geq D_k, \forall k \in \mathcal{K} \quad (17a)$$

$$E_k(m) - \sum_{t=1}^m a_k(t) (1 - \xi_k(t)) P_k \Delta\tau \geq \varepsilon_k, \forall k \in \mathcal{K}, m \in \mathcal{M} \quad (17b)$$

$$\|\mathbf{q}(t) - \mathbf{q}(t-1)\| \leq \nu_{h,max} \Delta\tau, \forall t \in \mathcal{M} \quad (17c)$$

Problem (17) is a non-convex problem due to the non-convex objective function and constraints. To deal with the non-convex item in E_f , we introduce a slack variable $s(t) \geq 0$ as (18).

$$s(t) = \left(\sqrt{1 + \frac{(\nu_h(t))^4}{4(\nu_0)^4}} - \frac{(\nu_h(t))^2}{2(\nu_0)^2} \right)^{\frac{1}{2}} \quad (18)$$

where $\nu_h(t) = \frac{\|\mathbf{q}(t) - \mathbf{q}(t-1)\|}{\Delta\tau}$ represents the horizontal flight speed within $Slot_t$. Therefore, E_f can be re-formulated as (19).

$$\begin{aligned} E_f(\mathbf{Q}, s(t)) \\ = \sum_{t=1}^M \Delta\tau \left(\frac{1}{2} d_0 \rho_s G (\nu_h(t))^3 + P_0 \left(1 + \frac{3(\nu_h(t))^2}{U_{tip}^2} \right) + P_1 s(t) \right) \end{aligned} \quad (19)$$

From (18), we can obtain (20).

$$\frac{1}{s(t)^2} = s(t)^2 + \frac{(\nu_h(t))^2}{(\nu_0)^2} \quad (20)$$

Let $s^r(t)$ as the r -th iteration of $s(t)$ and $v_h^r(t) = \frac{\|\mathbf{q}^r(t) - \mathbf{q}^r(t-1)\|}{\Delta\tau}$. Then, the first-order Taylor expansion of $s(t)$ at $s^r(t)$ can be denoted as (21).

$$\begin{aligned} s(t)^4 + s(t)^2 \frac{(\nu_h(t))^2}{\nu_0^2} &\geq \left(4s^r(t)^3 + 2s^r(t) \frac{(v_h^r(t))^2}{\nu_0^2} \right) s(t) \\ &- 3s^r(t)^4 - \frac{(s^r(t)v_h^r(t))^2}{\nu_0^2} \\ &\triangleq s^{lb}(t) \end{aligned} \quad (21)$$

Equation (17a) and (17b) is dealt in the same way. Let the r -th iteration of the UAV's trajectory $\mathbf{Q}^r = \{\mathbf{q}^r(t), \forall t \in \mathcal{M}\}$ and $\gamma_k \triangleq \frac{P_k \beta_0}{\sigma^2}$. The lower bound of $r_k(t)$ at $\|\mathbf{q}^r(t) - \mathbf{w}_k\|^2$ can be formulated as (22).

$$\begin{aligned} r_k(t) &\geq B \left(A_k^r(t) - I_k^r(t) \left(\|\mathbf{q}(t) - \mathbf{w}_k\|^2 - \|\mathbf{q}^r(t) - \mathbf{w}_k\|^2 \right) \right) \\ &\triangleq r_k^{lb}(t) \end{aligned} \quad (22)$$

where $A_k^r(t)$ and $I_k^r(t)$ are formulated as follows.

$$A_k^r(t) = \log_2 \left(1 + \frac{\gamma_k}{\|\mathbf{q}^r(t) - \mathbf{w}_k\|^2 + H^2} \right) \quad (23)$$

$$I_k^r(t) = \frac{\gamma_k \log_2 e}{\left(\|\mathbf{q}^r(t) - \mathbf{w}_k\|^2 + H^2 + \gamma_k \right) \left(\|\mathbf{q}^r(t) - \mathbf{w}_k\|^2 + H^2 \right)} \quad (24)$$

In the r -th iteration, both $A_k^r(t)$ and $I_k^r(t)$ are constant. For (17b), the lower bound of $h_k(t)$ at $\|\mathbf{q}^r(t) - \mathbf{w}_k\|^2$ can be formulated as (25).

$$\begin{aligned} h_k(t) &\geq \beta_0 \left(B_k^r(t) - (B_k^r(t))^2 \left(\|\mathbf{q}(t) - \mathbf{w}_k\|^2 - \|\mathbf{q}^r(t) - \mathbf{w}_k\|^2 \right) \right) \\ &\triangleq h_k^{lb}(t) \end{aligned} \quad (25)$$

where $B_k^r(t)$ is formulated as follows.

$$B_k^r(t) = \frac{1}{\|\mathbf{q}^r(t) - \mathbf{w}_k\|^2 + H^2} \quad (26)$$

In the r -th iteration, $B_k^r(t)$ is a constant. With $s^{lb}(t)$, $r_k^{lb}(t)$

and $h_k^{lb}(t)$, problem (17) is re-formulated as (27).

$$\min_{\mathbf{Q}, \{s(t)\}} E_f(\mathbf{Q}, s(t)) \quad (27)$$

$$s.t. s^{lb}(t) \geq 1 \quad (27a)$$

$$\sum_{t=1}^M a_k(t) r_k^{lb}(t) (1 - \xi_k(t)) \Delta\tau \geq D_k, \forall k \in \mathcal{K} \quad (27b)$$

$$\sum_{t=1}^m \eta a_k(t) P_U h_k^{lb}(t) \xi_k(t) \Delta\tau - \sum_{t=1}^m a_k(t) (1 - \xi_k(t)) P_k \Delta\tau \geq \varepsilon_k, \quad (27c)$$

$$\forall k \in \mathcal{K}, m \in \mathcal{M} \quad (27d)$$

Note that now both the optimization objective and constraints are convex with \mathbf{Q} and $s(t)$. Then, problem (27) is a convex optimization problem that can be solved by standard convex optimization solvers.

B. Optimization of IoT Devices' Scheduling

For any given and feasible UAV's trajectory $\mathbf{Q} = \{\mathbf{q}(t), t \in \mathcal{M}\}$ and charging fractions $\Xi = \{\xi_k(t), k \in \mathcal{K}, t \in \mathcal{M}\}$, energy consumption of the UAV for flight E_f is a constant. Meanwhile, the integer optimization variable $a_k(t)$ needs to be converted to a constant variable. Thus, the subproblem can be formulated as (28).

$$\min_A E_c \quad (28)$$

$$s.t. 0 \leq a_k(t) \leq 1, \forall k \in \mathcal{K}, t \in \mathcal{M} \quad (28a)$$

$$\sum_{k=1}^K a_k(t) \leq 1, \forall t \in \mathcal{M} \quad (28b)$$

$$\sum_{t=1}^M a_k(t) r_k(t) (1 - \xi_k(t)) \Delta\tau \geq D_k, \forall k \in \mathcal{K} \quad (28c)$$

$$E_k(m) - \sum_{t=1}^m a_k(t) (1 - \xi_k(t)) P_k \Delta\tau \geq \varepsilon_k, \forall k \in \mathcal{K}, m \in \mathcal{M} \quad (28d)$$

Note that now both the optimization objective and constraints are convex with $A = \{a_k(t), k \in \mathcal{K}, t \in \mathcal{M}\}$. Then, problem (28) is a LP (Linear Programming) problem that can be solved by standard convex optimization solvers. Due to the slackness of $a_k(t)$, the $a_k(t)$ obtained by solving problem (28) is constant, which has to be reconstructed. Each time slot needs to be divided into n sub-slots so that the total number of sub-slots is $N = nM, n \geq 1$. Then, the number of sub-slots allotted to UE_k in $Slot_t$ is $N_k(t) = \lfloor na_k(t) \rfloor$ where $\lfloor x \rfloor$ denotes the nearest integer of x [16].

C. Optimization of IoT Devices' Charging Fraction

For any given and feasible UAV's trajectory $\mathbf{Q} = \{\mathbf{q}(t), t \in \mathcal{M}\}$ and IoT devices' scheduling

$A = \{a_k(t), k \in \mathcal{K}, t \in \mathcal{M}\}$, E_f is constant. Thus, the subproblem can be formulated as (29).

$$\min_{\Xi} E_c \quad (29)$$

$$s.t. 0 \leq \xi_k(t) \leq 1, \forall k \in \mathcal{K}, t \in \mathcal{M} \quad (29a)$$

$$\sum_{t=1}^M a_k(t) r_k(t) (1 - \xi_k(t)) \Delta\tau \geq D_k, \forall k \in \mathcal{K} \quad (29b)$$

$$E_k(m) - \sum_{t=1}^m a_k(t) (1 - \xi_k(t)) P_k \Delta\tau \geq \varepsilon_k, \forall k \in \mathcal{K}, m \in \mathcal{M} \quad (29c)$$

It can be seen that both the optimization objective and constraints are linear. Thus, problem (29) is a LP problem that can be solved by standard convex optimization solvers.

D. Overall Algorithm

The formulated problem can be addressed with the proposed algorithm described in Figure 2.

Input: $A^0, \Xi^0, r = 0, \varepsilon, r_{max}$;
Output: Q^*, A^* and Ξ^* ;
while $\left| \frac{E_{cons}^r - E_{cons}^{r-1}}{E_{cons}^{r-1}} \right| > \varepsilon$ and $r \leq r_{max}$, **do**
 Solve subproblem (27) for given $\{A^r, \Xi^r\}$ and obtain Q^{r+1} ;
 Solve subproblem (28) for given $\{Q^{r+1}, \Xi^r\}$ and obtain A^{r+1} ;
 Solve subproblem (29) for given $\{Q^{r+1}, A^{r+1}\}$ and obtain Ξ^{r+1} ;
 Update $r = r + 1$;
end
return Q^*, A^* and Ξ^* .

Figure 2. Iterative optimization algorithm for solving problem (16).

First of all, feasible initial values $\{A^0, \Xi^0\}$ are given along with iteration precision ε and maximum iterations number r_{max} . Problem (27) is a convex problem, which can be solved by standard convex optimization solvers to obtain Q^{r+1} . With the obtained trajectory and current charging fractions $\{Q^{r+1}, \Xi^r\}$, the LP problem (28) can also be solved by standard convex optimization solvers to get the optimized scheduling variable. At last, the optimized charging fraction Ξ^{r+1} is obtained by solving problem (29) with $\{Q^{r+1}, A^{r+1}\}$. The r -th optimization results $\{Q^{r+1}, A^{r+1}, \Xi^{r+1}\}$ are obtained when the iteration is finished. Then, update the iteration number and check if it meets the ending conditions. If not, it should enter the next iteration until the iteration is over. Then, the optimal UAV's trajectory Q^* , communication scheduling A^* and charging fraction Ξ^* can be obtained. The computational complexity of the proposed algorithm is composed of three parts, i.e., solving problem (27), problem (28) and problem (29) using convex optimization solver based on the interior-point method. Given the solution accuracy of $\varepsilon > 0$ and the block coordinate descent complexity of $\log(\frac{1}{\varepsilon})$, the computational complexity of the proposed algorithm can be obtained as $\mathcal{O}((KM)^{3.5} \log^2(\frac{1}{\varepsilon}))$.

IV. SIMULATION RESULTS

This section will verify the effectiveness of the proposed algorithm for minimizing the energy consumption of UAV by simulation experiments and analyze the results. The UAV takes off from the starting position (-22,28,10) and returns to the starting position after a complete flight period. This paper assumes that the total data transmission requirements of all IoT devices are denoted by the vector $\mathbf{D} = 6.4 \times 10^8 \times [3, 12, 10, 7, 4, 15]^T$ bits. More details of the simulation parameters can be seen from the table I.

TABLE I
SIMULATION PARAMETERS

Parameter	Value
B	100 MHz
σ^2	1×10^{-7} W
β_0	1×10^{-2}
P_k	9×10^{-6} W
M	120
ε_k	1×10^{-6} J
P_U	5W
η	0.7
P_0	79.86
P_1	88.628
U_{tip}	120
v_0	4.03
ρ	1.225
s	0.05
G	0.503
d_0	0.6
$V_{h,max}$	6 m/s

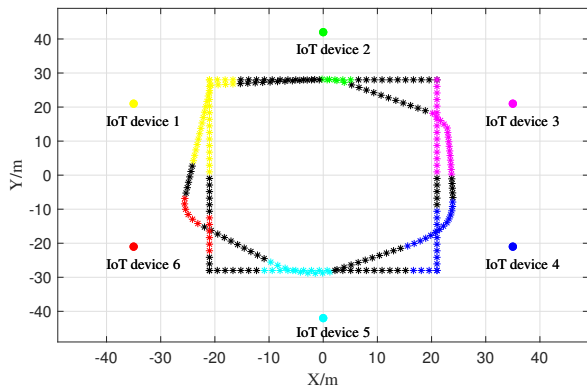


Figure 3. UAV's original trajectory and optimized trajectory.

Figure 3 shows the comparison of the initial trajectory (rectangle in the figure) and the optimized trajectory of the UAV when the flight period of the UAV is set to 40 seconds. From Figure 3, we can see that six IoT devices are evenly distributed in the map area as shown in the figure, and each device is represented by different colors. From Figure 3, it can be seen that the flight trajectory of the UAV is composed of all dots. In the flight trajectory of the UAV, the trajectory of the same color as the device indicates that the corresponding device is scheduled in currently, while the black part indicates that no

device is scheduled. The following simulation diagrams also use the same representation. In Figure 3, the rectangular vertex sandwiched between device 1 and device 2 is the starting position of the UAV, so this position is also the most obvious point in the complete optimization trajectory. In general, from either the initial trajectory or the optimized trajectory, the UAV begins to provide services for the corresponding device when getting close and stop when it is far away.

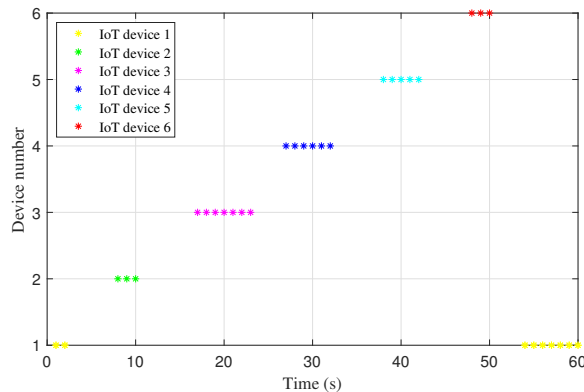


Figure 4. IoT devices' scheduling.

Figure 4 shows the communication scheduling of all IoT devices. It can be seen from Figure 4 that at the beginning of the flight period of the UAV, the first device to be scheduled is IoT device 1, which is scheduled again at the end of the flight period. This is because the flight starting position of the UAV is close to the IoT device 1 and when the UAV flight ends, it returns to the initial starting position. Therefore, it can be seen from the figure that except for IoT device 1 is scheduled twice, other devices have only one chance. It can also be seen from Figure 4 that at most one IoT device is scheduled at each time, which is consistent with the requirements in the system model.

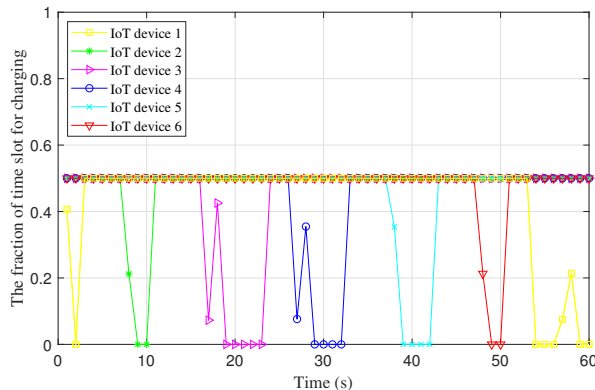


Figure 5. IoT devices' charging fraction.

Figure 5 shows the change of charging fraction of all IoT devices over time. Combining this figure with Figure 4, it can be seen that when an IoT device is scheduled, its effective

charging fraction varies from 0 to 0.5. When the device is not scheduled, its charging fraction is actually invalid, and the simulation results show that the values at this time are basically fixed at 0.5. It can also be seen from Figure 5 that IoT device 1 has two valid data of charging fraction, while other devices have only one. This is the same to the device's twice scheduling.

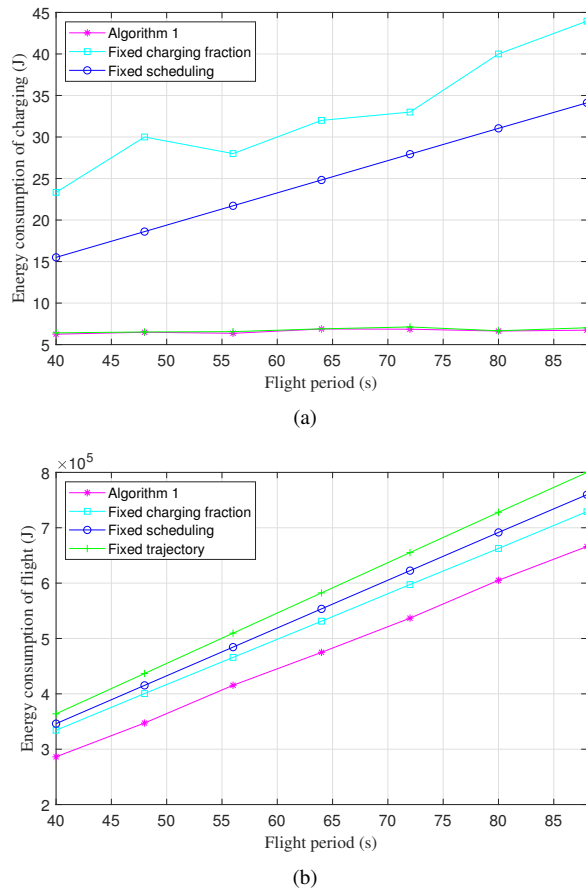


Figure 6. UAV's energy consumption: (a) energy consumption of flight, (b) energy consumption of charging.

Figure 6 shows the energy consumption of UAV, which mainly consists of energy consumption of the flight and the wireless charging. The two sub-diagrams in Figure 6 show the energy consumption changes relative to different flight periods. It can be seen from Figure 6(b) that with the increase of the flight period of UAV, the flight energy consumption of UAV also increases a lot. But compared with the fixed charging fraction, fixed communication scheduling variables and fixed trajectory, the optimization algorithm proposed in this paper can reduce the flight energy consumption of UAV effectively. It can be seen from Figure 6(a) that with the increase of the flight period, the energy consumption of the wireless charging of the UAV is increasing, but the optimization algorithm proposed in this paper can minimize the charging energy consumption subject to the constraints of data and energy.

V. CONCLUSION

This paper selects the data and energy integrated network based on UAV for in-depth research. The communication model of the system and the energy consumption model of ground IoT devices and the UAV are given. An energy-efficient resource allocation algorithm based on this scenario is proposed. The optimization objective is achieved by jointly optimizing of UAV trajectory, communication scheduling and wireless charging fractions of the ground IoT devices. At the end of this paper, the effectiveness of the proposed algorithm in minimizing the energy consumption of UAV is verified by multi-perspective simulation. As for future work, the multi-UAV scenario will be further studied in order to obtain better performance.

REFERENCES

- [1] A. Zanella, N. Bui, A. Castellani, L. Vangelista, and M. Zorzi, "Internet of things for smart cities," *IEEE Internet of Things journal*, vol. 1, no. 1, pp. 22–32, 2014.
- [2] A. Alrawais, A. Althothaily, C. Hu, and X. Cheng, "Fog computing for the internet of things: Security and privacy issues," *IEEE Internet Computing*, vol. 21, no. 2, pp. 34–42, 2017.
- [3] K. Wang, Y. Wang, Y. Sun, S. Guo, and J. Wu, "Green industrial internet of things architecture: An energy-efficient perspective," *IEEE Communications Magazine*, vol. 54, no. 12, pp. 48–54, 2016.
- [4] J. Wang *et al.*, "Taking drones to the next level: Cooperative distributed unmanned-aerial-vehicular networks for small and mini drones," *Ieee vehicular technology magazine*, vol. 12, no. 3, pp. 73–82, 2017.
- [5] Q. Wu *et al.*, "5g-and-beyond networks with uavs: From communications to sensing and intelligence, 2020," *arXiv preprint arXiv:2010.09317*.
- [6] Y. Du *et al.*, "Joint resources and workflow scheduling in uav-enabled wirelessly-powered mec for iot systems," *IEEE Transactions on Vehicular Technology*, vol. 68, no. 10, pp. 10 187–10 200, 2019.
- [7] X. Li *et al.*, "A near-optimal uav-aided radio coverage strategy for dense urban areas," *IEEE Transactions on Vehicular Technology*, vol. 68, no. 9, pp. 9098–9109, 2019.
- [8] Y. Sun, D. Xu, D. W. K. Ng, L. Dai, and R. Schober, "Optimal 3d-trajectory design and resource allocation for solar-powered uav communication systems," *IEEE Transactions on Communications*, vol. 67, no. 6, pp. 4281–4298, 2019.
- [9] J. Wang *et al.*, "Joint uav hovering altitude and power control for space-air-ground iot networks," *IEEE Internet of Things Journal*, vol. 6, no. 2, pp. 1741–1753, 2018.
- [10] M. Hua, L. Yang, Q. Wu, and A. L. Swindlehurst, "3d uav trajectory and communication design for simultaneous uplink and downlink transmission," *IEEE Transactions on Communications*, vol. 68, no. 9, pp. 5908–5923, 2020.
- [11] M. M. U. Chowdhury, S. J. Maeng, E. Bulut, and I. Güvenç, "3-d trajectory optimization in uav-assisted cellular networks considering antenna radiation pattern and backhaul constraint," *IEEE Transactions on Aerospace and Electronic Systems*, vol. 56, no. 5, pp. 3735–3750, 2020.
- [12] J. Hu, K. Yang, G. Wen, and L. Hanzo, "Integrated data and energy communication network: A comprehensive survey," *IEEE Communications Surveys & Tutorials*, vol. 20, no. 4, pp. 3169–3219, 2018.
- [13] L. Chiaraviglio *et al.*, "Bringing 5g into rural and low-income areas: Is it feasible?" *IEEE Communications Standards Magazine*, vol. 1, no. 3, pp. 50–57, 2017.
- [14] Q. Zhang *et al.*, "Distributed laser charging: A wireless power transfer approach," *IEEE Internet of Things Journal*, vol. 5, no. 5, pp. 3853–3864, 2018.
- [15] H. Mei, K. Yang, Q. Liu, and K. Wang, "Joint trajectory-resource optimization in uav-enabled edge-cloud system with virtualized mobile clone," *IEEE Internet of Things Journal*, vol. 7, no. 7, pp. 5906–5921, 2019.
- [16] Q. Wu, Y. Zeng, and R. Zhang, "Joint trajectory and communication design for multi-uav enabled wireless networks," *IEEE Transactions on Wireless Communications*, vol. 17, no. 3, pp. 2109–2121, 2018.